

An Automated Filter Bank-Based Pavement Crack Detection System Incorporating Standard Compression Coders

Clyde A. Lettsome¹⁺ and Yichang (James) Tsai²

Abstract: Wavelets/filter banks have become a popular area of research, especially in pavement distress, because they can be used concurrently to separate the subbands of signal frequencies and analyze the data in time/spatial domains. Because of this, filter banks have been studied in automated pavement distress detection and distress segmentation systems research. However, incorporating standard compression coders like Set Partitioning in Hierarchical Tree (SPIHT) or Joint Photographic Experts Group 2000 (JPEG2000) into automated filter bank-based distress detection and segmentation systems has not been presented. An automated filter bank-based pavement crack detection system that can effectively incorporate Standard Compression Coders into a filter bank-based automated crack detection and segmentation system has been proposed in this paper. This is the first known attempt to incorporate standard coders into a system. The proposed system has been validated using real pavement images provided by the Georgia Department of Transportation (GDOT). Preliminary results show that the proposed system can provide usable segmentation results, even at a low bit rate. This allows researchers to reduce data storage requirements and, most importantly, increase the speed over the Embedded Zero-tree Wavelet (EZW) used in previous filter bank-based automated pavement distress systems. Future research is also discussed.

Key words: Filter bank; JPEG2000; Low bit rate; Pavement crack detection, Pavement distress segmentation, Said Pearlman SPIHT Coder, Wavelet.

Introduction

In image processing, filtering and separating noise from a desired image is an important process. For example, when images are captured by cameras, undesirable data such as atmospheric gases and transistor noise are also captured. In the case of space observation, atmospheric gases may cause observed objects to appear distorted when captured by a camera. In addition to this, transistor noise within a camera can introduce noise. To create better images, the removal of atmospheric noise and transistor noise from images is highly desired.

When pavement images are captured, pavement distress is embedded in surface textural information (noise). For pavement distress detection, it is important that filtering techniques extract pavement distresses from surface textural information. This requires using filters to reduce surface textural information while preserving pavement distress information, which must be done concurrently. However, there are obstacles to reducing surface textural noise and preserving pavement distress. Take for example Fig. 1. In this image, the most prominent feature is surface textural information. The surface textural noise and pavement distress data are both high-frequency information; hence, to a highpass filter, both have similar frequency response characteristics. Therefore, reducing surface textural data will lead to some loss of pavement distress data. This means surface textural data must be removed carefully to ensure that sufficient pavement distress data remains.

One method proposed to aid with pavement distress analysis is the use of filter banks. The origination of filter banks can be attributed to multi-rate processing, which was first introduced by Schafer [1]. Later, in 1976, Crochiere, Webber, and Flanagan [2] introduced the first subband coding structure, which was intended for audio coding. Filter banks were later extended to two-dimensional applications by Vetterli [3-4]. His work led to filter banks being used for many imaging applications. Later, Woods and O'Neil [5] were able to show that filter banks can be effectively used to provide better quality than Discrete Cosine Transform (DCT)-based coders.

These contributions and, more specifically, the work of Woods and O'Neil, showed filter banks could be used as a tool for many applications. Since then, filter banks have been used in many image applications, including image compression [6-8], image enhancement and denoising [9], image interpolation [10], water-marking [9], and other applications [11].

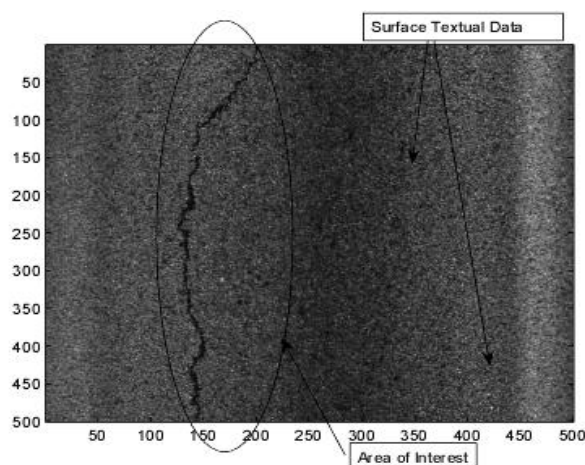


Fig. 1. Image of Pavement Containing Distress.

¹ School of Civil and Environmental Engineering, Georgia Institute of Technology, Atlanta, Georgia 30332, USA.

² School of Civil and Environmental Engineering, Georgia Institute of Technology, 210 Technology Circle, Savannah, GA, USA.

⁺ Corresponding Author: E-mail gtg955c@gatech.edu

Note: Submitted December 3, 2010; Revised November 7, 2011; Accepted November 9, 2011.

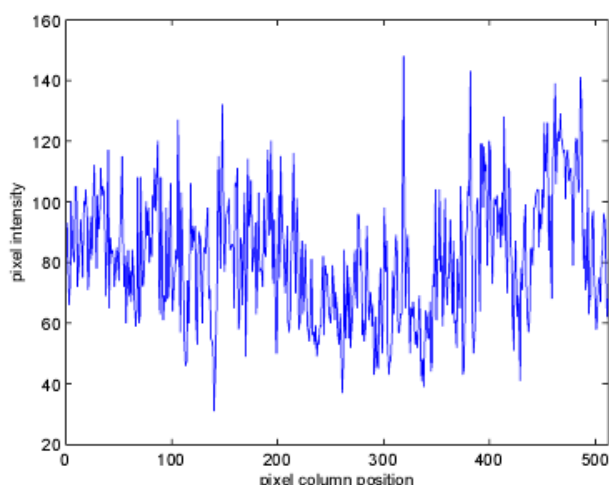


Fig. 2. Row 140 of Fig. 1 Prior to Noise Removal.

Researchers have extended the application of filter banks to pavement engineering and pavement distress problems [12-16]. For example, in automated pavement distress, filter banks can be used to compress, detect, isolate, and quantify cracks. In these applications, access to subband data is required. In compression applications, subband data is compressed and decompressed by using a compression codec. In the image processing community, the Joint Photographic Experts Group 2000 (JPEG2000) codec is considered to be the standard. In the case of crack detection, isolation, and quantification, thresholding is used to detect, isolate, and quantify cracks in pavement images and video. In all these cases, wavelets/filter banks have proven very useful.

Wavelets/filter banks have captured most researchers' attention in pavement engineering for two main reasons. First, unlike Fourier and DCT transforms, filter banks allow researchers to analyze any image in both the frequency and spatial domain. This is extremely attractive when analyzing complex signals. The second and probably the most attractive feature of filter banks is their ability to aid with image and data compression. For these reasons, many researchers have favored applying filter bank approaches to even more pavement imaging problems. This has also led to the misuse of wavelets/filter banks in some pavement imaging applications.

Although there has been some success with pavement image compression [15] and filter bank-based pavement distress detection [3], minimal advances have been made with incorporating the two into one system and developing a filter bank-based pavement segmentation approach [17]. This is because of how they have been applied in the past.

In previous automated pavement distress systems, Embedded Zero-tree Wavelet (EZW) was often the compression method of choice because EZW is flexible with respect to the filters used in the system. This can be useful when analyzing subband data for detection, isolation, and quantification but causes problems with overall system speed and compressed data size. By rearranging previously proposed filter bank-based pavement systems, it is possible to incorporate standard compression coders that increase system speed, improve compression rate, and maintain data integrity at low bit rates. By adding standard compression coders, state

Department of Transportations (DOTs) can save storage space, save data faster, and transmit large quantities of real-time data back to a lab with little loss in visual quality. For data transmission, compressed data can effectively be transmitted to remote facilities that house super computers, where significant amounts of pavement data can be processed rapidly and in near real-time.

In this paper, we analyze popular filter bank-based pavement distress detection systems. We discuss both the strengths and weaknesses of filter banks to aid in the successful application of the technology. Suggestions are made for improvements to filter bank-based pavement distress detection methods, specifically for better edge detection. We suggest reordering the steps for filter bank-based pavement distress detection systems so that standard compression coders can be used.

In Section 2, we explore the information that can be extracted from subband information by presenting an analysis of filter banks and current filter bank-based pavement distress issues. Section 3 provides a description of the step rearrangement and methods for applying different tools to exploit the available information to improve pavement distress detection and compression. Conclusions are summarized in Section 4.

Analysis of Current Filter Bank-Based Pavement Distress Issues

The goal of a pavement distress detection system is to extract pavement distress from a pavement image. Chambon *et al.* [16] defined a crack (distress) to be "a set of pixels that is darker than the background (textural surface pixels)." Moreover, they defined a crack to be "a set of connected small segments of different orientations." Using this definition, it is evident that the region labeled "area of interest" in Fig. 1 contains distress. However, because of the large amount of textural information, it is difficult to identify crack pixels in Fig. 2, which is row 140 from Fig. 1. Crack identification is essentially impossible without prior knowledge of the location. This is the challenge researchers experience when performing crack detection on pavement distress images. Filter bank analysis is performed in 1-dimension at a time with separable filters on input images. Therefore, it is challenging to extract crack data from surface textural data because surface textural data outnumber crack data. Furthermore, both crack and surface textural data exhibit many of the same characteristics.

Distress Detection and Surrounding Issues

For filter bank-based pavement distress detection systems, there has been one generally adopted approach based on subband coding information [14, 18-20]. Rather than using the Fourier transform, Zhou [14], preferred filter banks as a tool because of their ability to represent any signal as a set of finite length "waves" that can be used for pavement distress detection. These finite waves are subband coded data. The following introduces the common filter bank structure.

Because of its simplicity and effectiveness, the most common structure for many filter bank applications is the two-band structure illustrated in Fig. 3.

Filter bank-based systems are based on the multi-rate equation

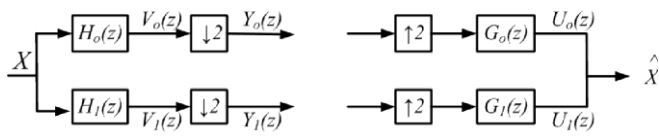


Fig. 3. Two-band Analysis-synthesis Filter Bank.

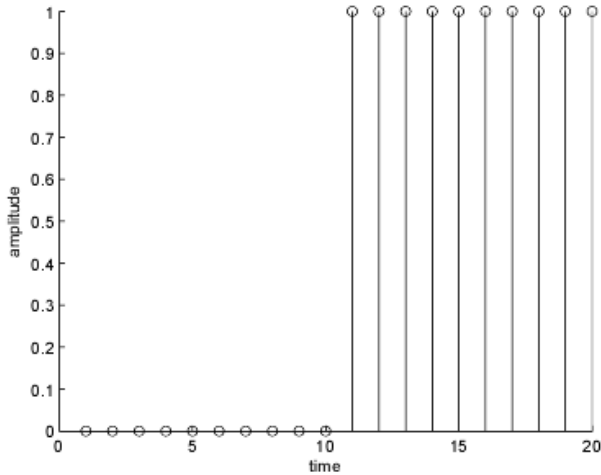


Fig. 4. Unit Step Function.

[21] for a two-band structure written in the z -domain as

$$\hat{X} = \frac{1}{2} X(-z)[H_o(-z)G_o(z) + H_1(-z)G_1(z)] + \frac{1}{2} X(z)[H_o(z)G_o(z) + H_1(z)G_1(z)] \quad (1)$$

where X is the input and \hat{X} is the reconstructed output. There are two components associated with this equation. They are the aliasing component given by

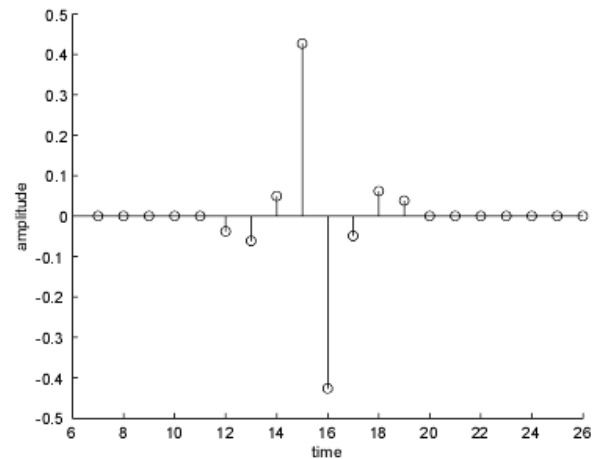
$$\frac{1}{2}[H_o(-z)G_o(z) + H_1(-z)G_1(z)] \quad (2)$$

and the transfer function term

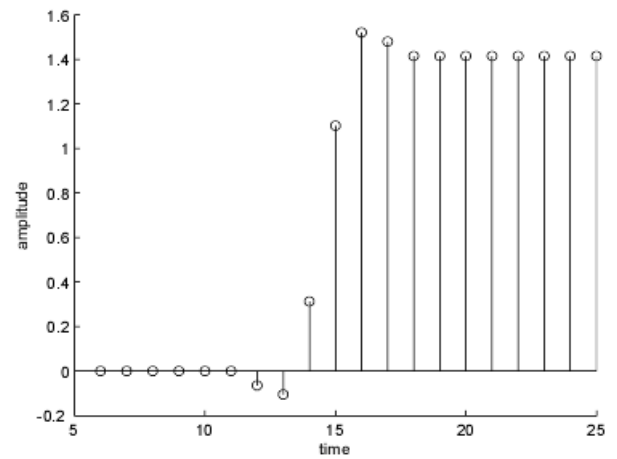
$$\frac{1}{2}[H_o(z)G_o(z) + H_1(z)G_1(z)] \quad (3)$$

When the filter coefficients in H and G are correctly chosen, the filter bank's alias function reduces to zero, and the transfer function term is unity. This leads to exact reconstruction (ER) [22] for the system in Fig. 3.

For images, the analysis subsystem on the left divides the input into four frequency subbands: HH_k , HL_k , LH_k , and LL_k , where H denotes highpass (H) frequency filtering and L denotes lowpass (L) filtering. The first letter in the subband notations represents the filtering performed horizontally, and the second represents the filtering performed vertically. The subscript k represents the level of decomposition in an octave-band coded system. The synthesis subsystem, on the right side of Fig. 3, recombines each subband so that a representation of the original signal is reproduced.



(a)



(b)

Fig. 5. Unit Step Function after Filtering (a) Filtered with a Daubechies Synthesis 9-tap Highpass Filter; (b) Filtered with a Daubechies Synthesis 7-tap Lowpass Filter.

If this procedure is used on a pavement image, pavement distress and surface textural data would manifest themselves in the form of non-zero values, or waves, in each subband containing highpass information. Current distress detection methods determine or segment distresses by comparing the non-zero values in the highpass subbands to a predetermined threshold. Any value larger than the threshold is possible pavement distress. Because of the simplicity and ability of the approach, it is highly attractive. However, there are two issues that plague this pavement distress detection method. First, comparing the highpass data to a threshold to determine a distress could be problematic. Second, downsampling will add some distortion to the results.

To better understand the first issue surrounding a threshold-based pavement distress detection method that uses highpass subband information, consider this method on the step function shown in Fig. 4. When it is filtered by the Daubechies synthesis filter coefficients [23], the highpass and lowpass subband results are shown in Fig. 5(a) and 5(b).

The lowpass channel is a scaled version of the original step function, while the highpass channel shows a "wavelet" that can be

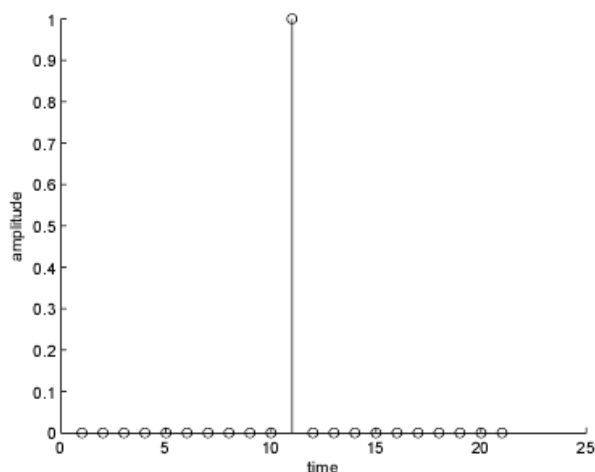
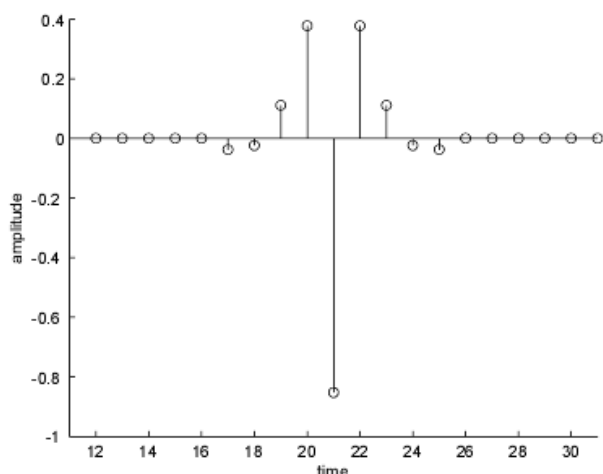
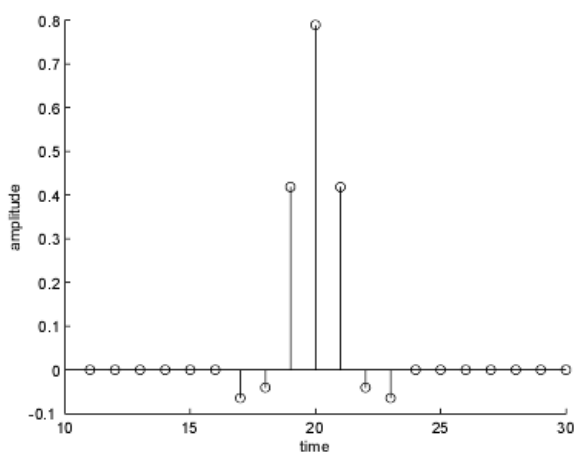


Fig. 6. Unit Impulse Function.



(a)



(b)

Fig. 7. Unit Impulse Function after Filtering (a) Filtered with a Daubechies Synthesis 9-tap Highpass Filter; (b) Filtered with a Daubechies Synthesis 7-tap Lowpass Filter.

used to help localize the area of discontinuity (edge) in a given signal. The local minimum and the local maximum values in Fig.

5(a) indicate the area of discontinuity for the step function. For this example, a threshold is set at ± 0.4 . Therefore, only two values meet these thresholds. Although this indicates the edge, this is a very simple example, and closer analysis of the method makes it apparent why this method is not the best one to use when combining it with a threshold to find a discontinuity.

The impulse response shown in Fig. 6 contains two areas of discontinuity about $t=11$.

Because these two areas are within close proximity, non-zero values in the highpass channel associated with each region of discontinuity will Overlap and Add (OLA), as shown in Fig. 7, and will be composed differently from the non-zero values illustrated in Fig. 4. It is possible to see that there are three values equal to or less than -0.4 . Furthermore, there is now a value of -0.8 . This leaves the user with the dilemma of choosing between ± 0.4 or ± 0.8 as the appropriate threshold.

Thus far, only 1-dimensional signals have been illustrated. However, pavement distress detection on images is a 2-dimensional process. This means the OLA, experienced because of the close proximity of discontinuities, is further amplified when the second dimension is considered. Both of these facts lead to significant false positives and false negatives in pavement distress detection.

A second and lesser reason for the filter banks' poor performance for pavement distress detection is the sampling found in subband coding. This sampling leads to a loss of translation variance and produces large numbers of additional artifacts. This compounds the problems encountered when using a filter bank-based pavement distress detection system where thresholding is used on subband information.

Detection and Compression Solutions and the Trade-offs

In the literature, one method has been suggested for improving detection. Zhou [15] suggested reducing the filter lengths used in order to reduce OLA. However, reduction in filter length does not allow for the use of standard compression coders, such as the Said Pearlman (S+P) SPIHT coder [6] and JPEG2000 [7]. Instead, inferior compression methods such as the EZW are used at the expense of image quality, overall system speed, and final storage size. These coders use the Daubechies 9/7 filters, which are not short and contain a "tail" outside of the filters' main lobe. This leads to the OLA issue discussed in subsection 2.1. Furthermore, shorter filters do not allow for the proper channel separation needed for effective filter bank-based compression. Because of the OLA and channel separation issues, we propose a different approach to pavement distress detection in which pavement distress detection does not occur after decomposition but, instead, occurs in two steps. A preliminary statistical-based detection is performed before decomposition with a filter bank-based approach occurring after reconstruction. These approaches will not only be beneficial to improving detection, but will also be beneficial to filter bank-based pavement distress segmentation methods.

Restructuring Pavement Distress Detection Systems and Results

In this section, an improved pavement distress detection method is

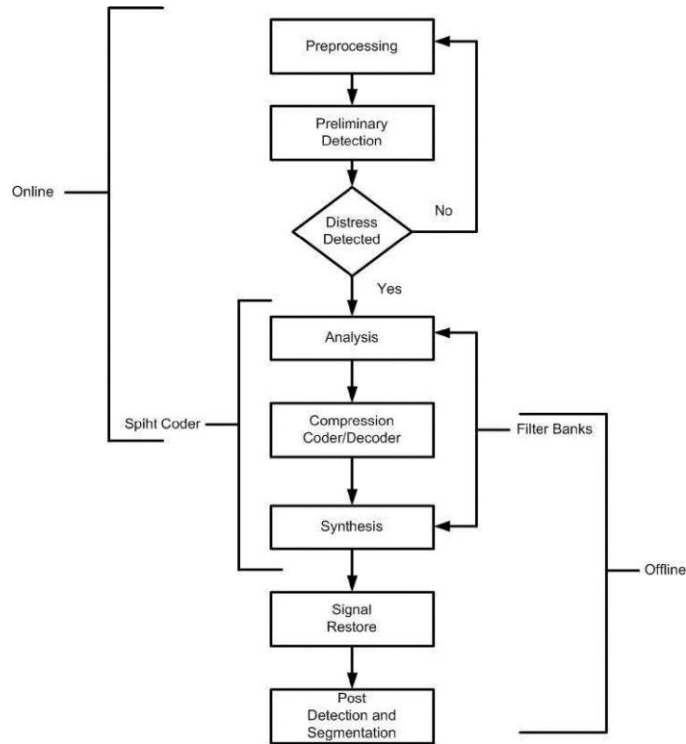


Fig. 8. Restructured Automated Pavement Distress Detection System.

proposed. This method will make it possible for filter bank-based pavement distress systems to use standard compression coders in the same system. The inverse correlation between compression and detection will be eliminated by uncoupling detection and compression so the detection process is moved from between the analysis and compression coder.

For the experiments, the S+P SPIHT coder that has long been established as one of the standard filter bank-based compression coders is employed. In the restructuring and reformulating of this system, certain assumptions are made. First, in order to focus on the main objective, the system will include a uniform artificial lighting source. By making this assumption, shadows on the pavement surface can be ignored. Also, pavement images that contain road markings will not be used. A diagram of a newly restructured system is illustrated in Fig. 8. This design is a restructured version of the system proposed by Zhou [14].

Preprocessing

Because surface textural information interferes with pavement distress detection, a method to reduce the impact of surface textural information that will isolate pavement distresses is proposed. This will isolate pavement distresses. A statistical-based approach similar to the one used by Rajan [24] is proposed.

For this statistical approach, the mean, \bar{X} , of the captured image is found where

$$\bar{x} = \frac{\sum_1^m \sum_1^n X_i(m,n)}{m*n} \tag{4}$$

and the variables m and n are the dimensions of the captured image

X_i . Using Eq. (4), the standard deviation(s) of a given image is determined using the equation

$$s = \sqrt{\frac{1}{m-1} \frac{1}{n-1} \sum_1^m \sum_1^n (X_i(m,n) - \bar{x})^2} \tag{5}$$

Then Eqs. (4) and (5) are used to approximate the bottom of the surface textural data (in the z direction of an image). This is based on the intensity data and the approximate location is given by the equation

$$L_{st} = \bar{x} - s \tag{6}$$

where L_{st} is the approximate lower location or approximate lowest intensity value of the surface textural data. To eliminate the surface textural data, the following logic is used to normalize values greater than L_{st} .

$$X_{pp}(m,n) = \begin{cases} \bar{x} & \text{if } [X_i(m,n) > \bar{x} - s \text{ and } X_i(m,n) > \bar{x}] \text{ or } [X_i(m,n) > \bar{x} - s] \\ X_{i(m,n)} & \text{otherwise} \end{cases} \tag{7}$$

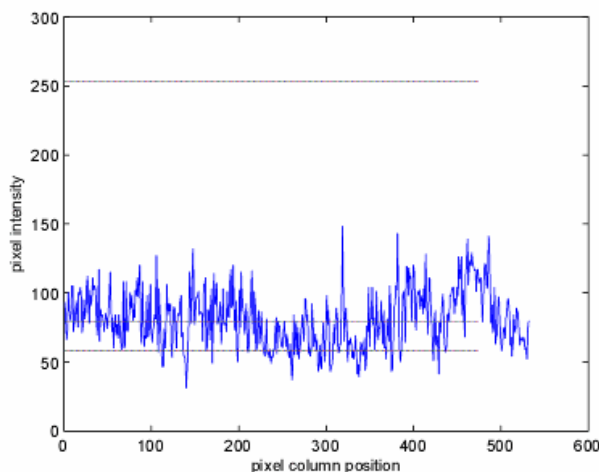
To better understand this, consider Fig. 1. This image has a mean of 79.22 and a standard deviation of 21.11. Using Eq. (6), the approximate location of the surface textural data is 58.11. With this information, surface textural data is normalized to the mean using Eq. (7). For a different view of this procedure, row 140 from Fig. 1 is selected. Fig. 9(a) shows the captured row's data, and Fig. 9(b) shows the preprocessed row after the normalization or surface textural removal. The result of this process on Fig. 1 is shown in Fig. 10.

It is clear that a significant amount of noise has been removed from the image; therefore, less noise will be stored in automated pavement distress detection systems.

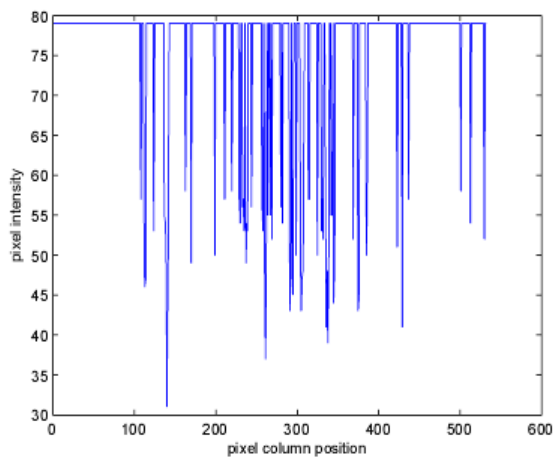
Distortion in the form of surface pavement discoloration and debris is not addressed with this method because in most cases, surface discoloration and surface debris will not change the mean or standard deviation significantly and, more importantly, surface discoloration will not affect distress values. Unless the discoloration penetrates the surface and protrudes into the pavement and is within close proximity to the pavement distress, the distress intensity will not be affected. Thus, these have little effect and are not considered in this analysis.

Repositioning Detection

In an effort to improve pavement distress detection while imposing less of a negative impact on compression, the pavement distress detection process is removed from between the analysis and compression coder. One option for a new location is to move the detection after the compression decoder and before the synthesis process. However, this solution can introduce a problem. If detection is performed after the compression decoder, the detection algorithm will be dependent on the highpass that has been eroded from high subbands due to compression, and the problem is only amplified as the compression rate is lowered. To see this, consider



(a)



(b)

Fig. 9. Illustration of Online Surface Texture Removal (a) Row 140 of Image Prior to Surface Texture Removal; (b) Row 140 of Image after Surface Texture.

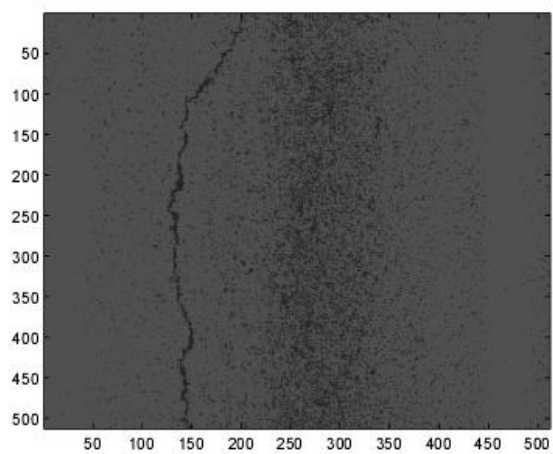
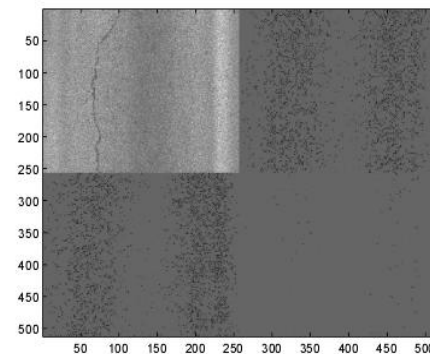
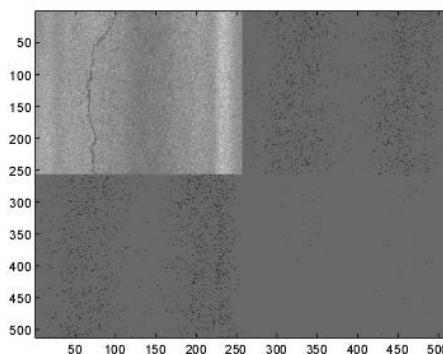


Fig. 10. Image Preprocessed to Surface Texture.

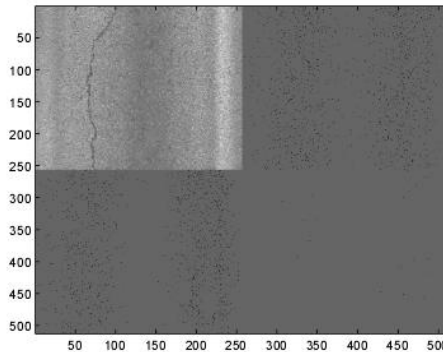
Fig. 11, which shows subband information for a sample image. This image has been decomposed to one level and has four subbands.



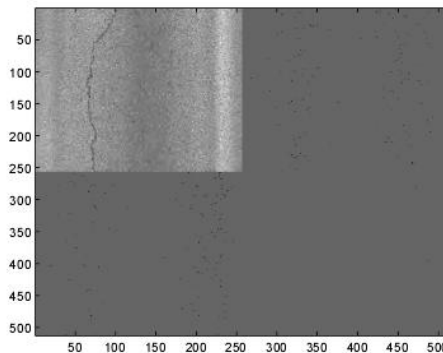
(a)



(b)



(c)



(d)

Fig. 11. Illustration of Image Subbands for Pavement Distress Image Coded at Four Different Bit-rates (a) 1 bpp; (b) 0.75 bpp; (c) 0.5 bpp; (d) 0.25 bpp.

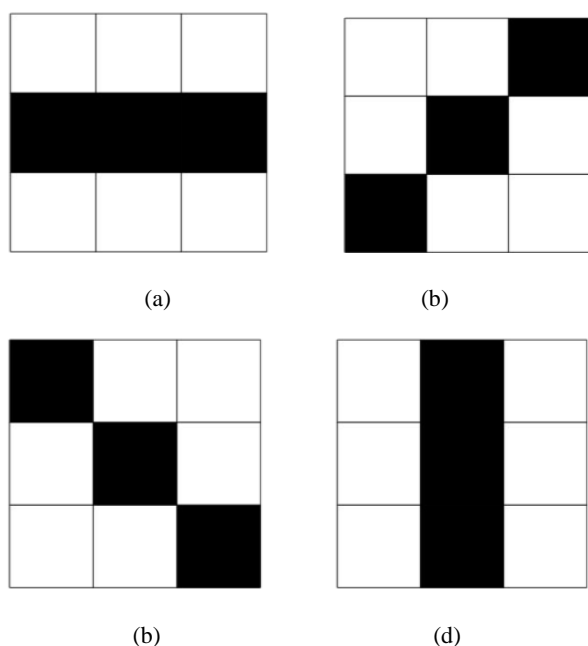


Fig. 12. Illustration of distress at different orientation (a) 0 degrees angle; (b) 45 degrees angle; (c) 135 degrees angle; (d) 90 degree angle.

Through close inspection, one can see that information in any subband containing highpass information is being eroded as the bit-rate is reduced. Thus, this approach is not suitable based on the design goals. Consequently, a two-step detection approach is utilized. One method is statistically based, and the other is filter bank-based. Both processes are positioned outside the entire filter bank system, as illustrated in Fig. 8. The first process is placed after the preprocessing step, while the second detection process is placed after the signal restoration step. The justification for both processes will be outlined in the following two subsections.

Preliminary Detection

The preliminary detection process incorporated into our method is computationally less expensive than Zhou's method [14]. This is simply based on the positioning of the detection method. This detection method occurs before the analysis and, thus, it is not dependent on subband domain data. This means two things. First, detection is not affected by the OLA associated with the decomposition of an input image into subbands. Second, distress is detected without requiring numerous multiplies and adds associated with convolution in the decomposition of an image. That is to say, decomposition is not performed unless distress is suspected, as illustrated in Fig. 8. This potentially increases the speed of this approach, which is very attractive because this will be used online (in the field).

To effectively detect pavement distress, it is necessary to look at pavement distress from a 3-dimensional view even though the source is 2-dimensional. In Section 2, we discussed how much easier pavement distresses can be found using two-dimensional data and intensity instead of one-dimensional data and intensity, as done

in many filter bank-based pavement distress methods. Because of the difficulty associated with analyzing pavement distress in one and two dimensions, the proposed method approaches the distress detection process from a 3-dimensional point of view in which x and z are the image's width and length, and intensity represents an *approximation* for depth. The depth (intensity) cannot be considered alone. The intensity data of any given pixel becomes relevant when it is adjacent to data of similar intensity. Through inspection of a pavement distress image (such as Fig. 10), there are a few more characteristics that distinguish distress pixels from noise. Pavement distress appears to be more linear, while the noise appears to be more random. Finally, pavement distress often appears to be darker than other regions.

Utilizing this information, a 3x3 pixel window is employed in the pavement distress method to find dark, possibly linear distress situation regions. To define a dark pixel or distress, the equation

$$L_d \geq \bar{x} - 2s \tag{8}$$

is used where L_d represents distress intensity or location relative to 0 (intensity). When a pixel fitting this criterion is found, the 3x3 window is positioned above it so that the pixel is in the center of the window. Any dark pixel in the window is classified as part of a possible linear combination or an isolated dark spot. If surrounding pixels form any of the linear patterns found in Fig. 12, and their values satisfy Eq. (8), then there is a high probability that there is pavement distress.

Being "almost certain" that a distress is present, however, is not good enough. It may be necessary that a given distress threshold be met in each captured image to satisfy certain criteria for various pavement distresses. A common measure in pavement distress research has been the Universal Crack Index (UCI). From the available data, a measure similar to the UCI can be developed. To calculate this measure, which we call Percentage of Pavement Distress (PPD), a threshold must first be determined. This threshold is used as a pseudo-depth value that indicates a distress and is based on pixel intensity. This value can be any value larger than L_{st} . The pixel values from the preprocessed image, X_p , are binarized by using the following equation:

$$B_d(m,n) = \begin{cases} 1 & \text{if } X_p(m,n) < T_d \\ 0 & \text{otherwise} \end{cases} \tag{9}$$

where B_d indicates binarized pavement distress and T_d is the user's selected threshold. This threshold can be set to one (σ) or two (2σ) standard deviations below the overall image mean value. The Percentage of Pavement Distress is then calculated by the equation

$$PPD = \frac{\sum_1^m \sum_1^m B_d(m,n)}{m * n} \tag{10}$$

Based on the PPD results, the user can decide to classify the image as possibly containing or not containing distress.

Online Detection

Implementing a second distress detection method may seem

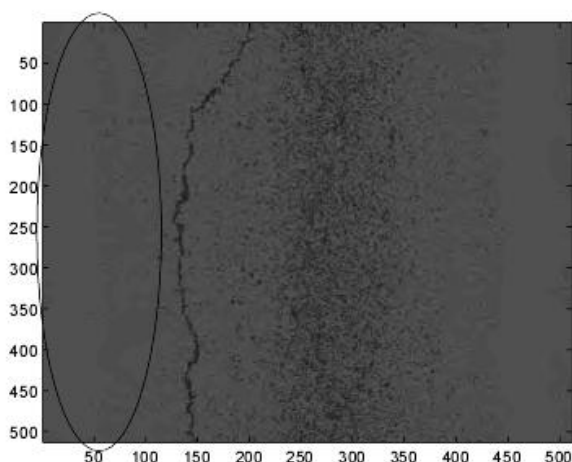


Fig. 13. Noise Reduction Due to 0.25 bpp Image Compression.

redundant, but this distress detection process assists the pavement distress segmentation method by assisting with the localization of pavement distress. The spatial and frequency data from filter banks can be useful for this localization. Some adjustments need to be made to the conventional subband coder to allow for its intended purposes.

We begin the adjustment by first recalling the multi-rate equation for a two-band structure written in the z -domain as

$$\hat{X} = \frac{1}{2} X(-z)[H_0(-z)G_0(z) + H_1(-z)G_1(z)] + \frac{1}{2} X(z)[H_0(z)G_0(z) + H_1(z)G_1(z)] \quad (11)$$

where $x[n]$ is the input and $\hat{x}[n]$ is the reconstructed output. There are two components associated with this equation. They are the aliasing component given by

$$\frac{1}{2}[H_0(-z)G_0(z) + H_1(-z)G_1(z)] \quad (12)$$

and the transfer function term

$$\frac{1}{2}[H_0(z)G_0(z) + H_1(z)G_1(z)] \quad (13)$$

Ideally, the filter bank's aliasing term should reduce to zero, and the transfer function term is unity. However, because our design criteria have changed, this is no longer true. We are no longer

1. designing a subband coder for multi-level decomposition,
2. designing a subband coder for compression,
3. concerned about channel separation necessary for multi-level decomposition,
4. in need of half-band filters,
5. in need of filters that add little distortion, or
6. in need of avoiding the loss of translation variance due to sampling [12].

Given these criteria, Haar filters that have been re-scaled are used to allow the transfer function to reduce to 0.5. This means the filter coefficients will be [0.5 0.5] for the lowpass filter coefficients and

[0.5 -0.5] for the highpass filter coefficients. The highpass filters can be used with a segmentation algorithm to detect and segment pavement distress with little distortion.

Image Restoration

Now that the pavement distress detection has been uncoupled from the compression, it is possible to achieve higher compression rates, however determining the amount of compression that can be tolerated is also necessary. After compression and reconstruction of a signal in any lossy system, as with automated pavement distress systems, the output signal is not equivalent to the input signal ($X \neq \hat{X}$). This means any analysis of the output signal, \hat{X} , is performed on distorted data. Unfortunately, compression coders are not linear, and, thus, the original input signal cannot be reconstructed. However, some data may be restored by using the type of data that is most vulnerable.

As bit-rate is lowered, isolated pixels and pixels closest to zero (in this system, values closest to the mean) are most affected. This has both positive and negative consequences. Because noise is usually isolated and random, noise is affected more as the bit-rate is lowered and is, thus, a good consequence of lowering bit-rate. This noise reduction due to compression can be seen when Fig. 13 is compared to Fig. 10.

However, as the bit-rate is lowered, pavement distress classified as hairline distress is also affected because hairline distress is relatively isolated and often is not as dark (hence less intense) as other pavement distresses. This means users must balance the importance of hairline distress detection and isolation with the need to eliminate noise and the need to compress images to allow efficient data storage.

Although, the compression algorithm eliminates high frequency noise, it also introduces some noise because of the loss of high frequency information. In effect, it creates a rippling distortion in areas where high-frequency information was removed or attenuated. This is similar to the Gibbs phenomenon encountered when a lowpass filter is used to filter areas of discontinuity. Through closer inspection of the highlighted region of Fig. 13, for example, there is a light but large area of gray that was not apparent in Fig. 10. This may be eliminated with the assistance of the mean and standard deviation found by the preprocessing discussed in Section 3.1. The distortion values are normalized by using the following rules:

$$X_{pp}(m,n) = \begin{cases} \bar{x} & \text{if } [\hat{X}_i(m,n) > \bar{x} - 0.5s \text{ and } \hat{X}_i(m,n) > \bar{x}] \text{ or } [\hat{X}(m,n) > \bar{x} - s] \\ X_{i(m,n)} & \text{otherwise} \end{cases} \quad (14)$$

Applying these rules to Fig. 13 yields the results seen in Fig. 14 removes some noise from the compressed image, making it closer in appearance to Fig. 10 with some additional surface textural information removed.

However, this also means that the statistical information, such as mean and standard deviation information for each image must be stored with the pavement distress image and GPS location.

Adding the signal restoration step would be optional. Usage will be based on other factors and design criteria, such as the type of segmentation algorithm used.

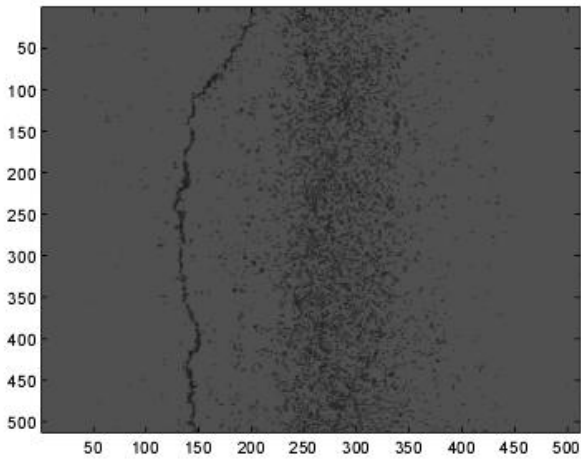


Fig. 14. Noise Reduction from Normalization.

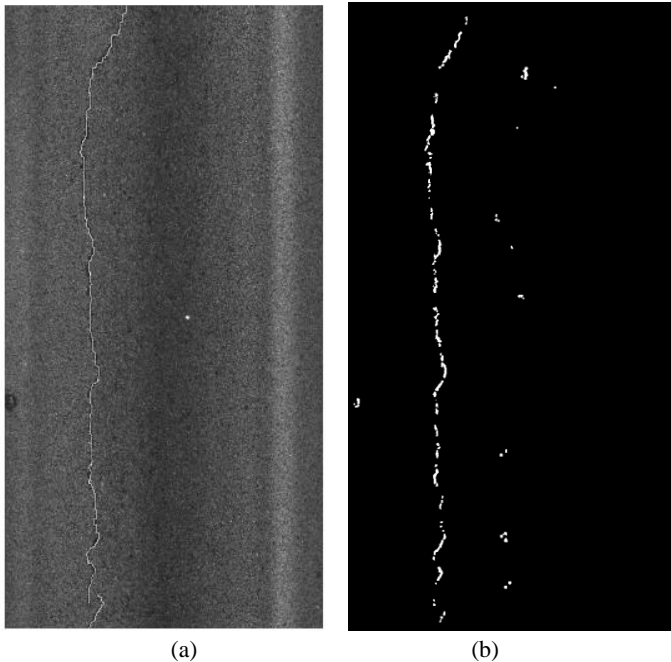


Fig. 15. New Pavement Distress Segmentation Method Performed on GADOT Image 1D579384: (a) Ground (b) S+P SPIHT Compressed Result at 0.25 bpp.

Test Results

Now that we have illustrated how standard compression coders can be incorporated into filter bank-based automated pavement distress systems, we will show some segmentation results. In this work, a filter bank-based segmentation method was proposed. However, other segmentation methods, such as Canny, Dynamic Optimization, and Iterative Clipping segmentation methods may be used to perform the segmentation. The proposed system has been further validated using real pavement images provided by the GDOT. Fig. 16(a) and 17(a) show the ground truth of two pavement distress images supplied by the GDOT. These images were compressed using the proposed system, segmentation was performed using the filter bank-based segmentation method, and the results are shown in

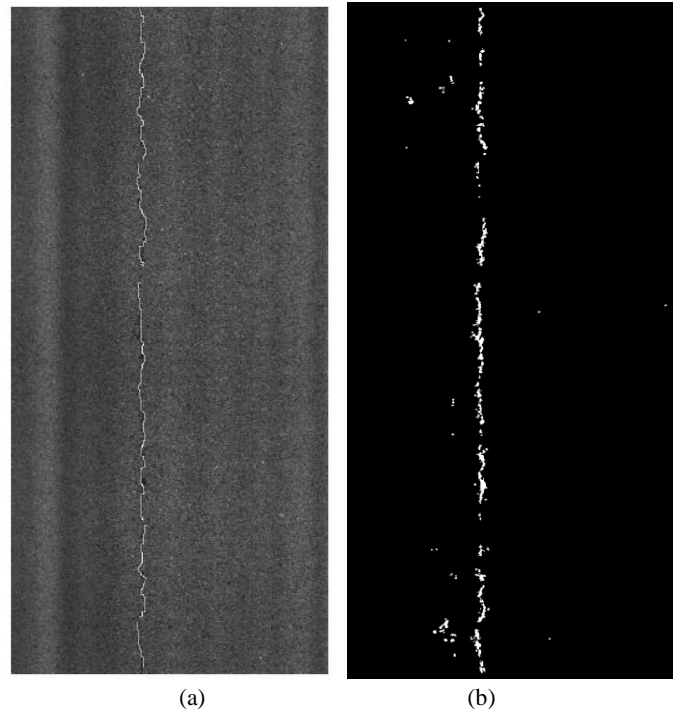


Fig. 16. New Pavement Distress Segmentation Method Performed on GADOT Image 1D560029: (a) Ground (b) S+P SPIHT Compressed Result at 0.25 bpp.

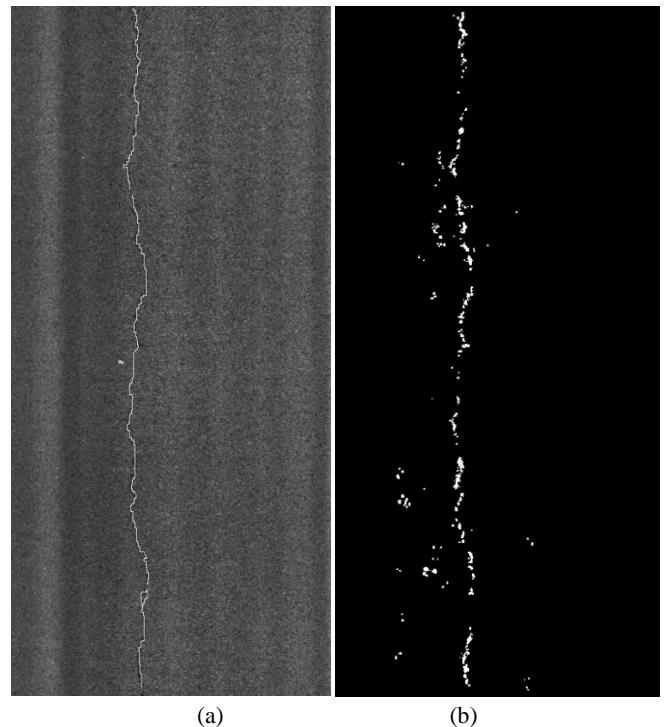


Fig. 17. New Pavement Distress Segmentation Method Performed on GADOT Image 1D560030: (a) Ground (b) S+P SPIHT Compressed Result at 0.25 bpp.

Figs. 16(b) and 17(b).

From these two results, the results mirror the ground truth closely despite the 0.25 bpp compression rate. Experiments were completed on additional GDOT images, and the quantitative results are shown

Table 1. Buffered Scoring Metric on the Compressed Image.

Image Identifier With Ground Truth	Restructured Filter Bank-Based System's Buffered Score	PSNR At 0.25 bpp
GDOT Image Reference #1D579384 (Fig. 15)	81.7983	25.25 db
GDOT Image Reference # #1D560029 (Fig. 16)	85.4362	26.93 db
GDOT Image Reference # #1D560030 (Fig. 17)	77.5191	26.71 db
GDOT Image Reference # #1D560076	45.5308	20.58 db
GDOT Image Reference # #1D560083	43.2553	26.46 db
GDOT Image Reference #1D560088	22.3997	25.43 db
GDOT Image Reference #1D560094	53.7399	24.98 db
GDOT Image Reference #1D560100	47.7607	25.39 db
GDOT Image Reference #1D560106	50.4041	25.34 db
GDOT Image Reference #1D560108	58.5084	26.24 db
GDOT Image Reference #1D560113	62.9191	24.02 db
GDOT Image Reference #1D560182	33.9334	22.94 db
GDOT Image Reference #1D560445	64.5736	28.91 db

in Table 1. A buffered scoring metric developed by Tsai *et al.* [17] was used to quantify the effectiveness of the method. For this metric, values of 1 to 100 are assigned to results with 100 being perfect segmentation and 1 being poor segmentation. The score for the filter bank-based segmentation method is shown in the table. In addition, the signal-to-noise ratio is given for each compressed image.

The preliminary results show that the proposed method can provide better segmentation results at a low bit rate. Because these standard coders yield better signal-to-noise ratios than EZW and enhanced EZW methods used previously in similar systems, less distortion is produced, thus helping many detection algorithms detect pavement distress that were not designed to be used on compressed images. Furthermore, this proposed system reduces data storage needs and, more importantly, it increases the speed of compression over the time required for the EZW [6] used in previous filter bank-based automated pavement distress systems.

Conclusions and Recommendations

In this paper, a new, automated filter bank-based pavement crack detection system is proposed. Unlike other known automated filter bank-based systems, the proposed method allows the standard compression coders to be used. To make this possible, we propose that online distress detection and quantification of pavement distress not depend on subband data for detection. This allows for a more accurate calculation of a crack index and removes the need for shorter filters so that standard compression coders like the Said Pearlman SPIHT coder and JPEG2000 that use longer filters can be incorporated into these systems. The proposed system has been further validated using actual pavement images provided by the GDOT. The preliminary results show that the proposed system allows for better offline reconstructed results at lower bit rates, which will lead to better segmentation results, as is shown in the experimental results. The findings in this work are preliminary and more comprehensive image testing is recommended. In future work, we will experiment with other techniques to improve the overall system speed and noise reduction capability, and we will use other proven edge detection methods. The proposed system has the potential to enhance existing image acquisition processes, one of the

important components in automated pavement distress detection, by allowing end users to use the standard encoders to compress images (reduce image processing and image storage size) while maintaining the distress detection accuracy. In addition, state DOTs could transmit large quantities of real-time images or video of pavement data to remote locations with little loss in signal quality. Tests can be conducted to measure the benefit of reducing processing time and storage.

Acknowledgments

The work for this paper was supported by the National Science Foundation. The authors owe thanks to the Georgia Department of Transportation for providing the actual pavement images for this study.

References

1. Rabiner, R.W. and Schafer, L.R. (1973). A Digital Signal Processing Approach to Interpolation, *Proceedings of the IEEE*, pp. 692-702.
2. Crochiere, R.E., Webber, S.A., and Flanagan, J.L. (1976). Digital Coding of Speech in Sub-Bands, *Bell Systems Technical Journal*.
3. Vetterli, M. (1984). Multi-Dimensional Subband Coding: Some Theory and Algorithms, *Signal Processing*, Vol. 6, pp. 91-112.
4. Wang, K.C.P., Qiang, L., and Weiguo, G. (2007). Wavelet-Based Pavement Distress Image Edge Detection with "À Trous" Algorithm, *Transportation Research Record*, No. 2024, pp. 73-81.
5. Woods, J. and O'Neil, S. (1986). Subband Coding of Images, *IEEE Transactions on Acoustics, Speech and Signal*, 34(5), pp. 1278-1288.
6. Said, A. and Pearlman, W.A. (1996). A New, Fast, and Efficient Image Codec Based on Set Partitioning in Hierarchical Trees, *IEEE Transactions on Circuits and Systems for Video Technology*, 6(3), pp. 243-250.
7. Skodras, A., Christopoulos, C., and Ebrahimi, T. (2001). The Jpeg 2000 Still Image Compression Standard, *IEEE Signal*

- Processing Magazine*, 18(5), pp. 36-58.
8. Mujica, F., Murenzi, R., Smith, M.J.T., and Leduc, J.-P. (1998). Robust Object Tracking in Compressed Image Sequences, *Journal of Electronic Imaging*, 7(4), pp. 746-754.
 9. Jung, C.R. and Scharcanski, J. (2004). Wavelet Transform Approach to Adaptive Image Denoising and Enhancement, *Journal of Electronic Imaging*, 13(2), pp. 278-285.
 10. Chen, B. and Latifi, S. (2000). Astronomical Image Manipulation in the Discrete Wavelet Transform Domain, *Journal of Electronic Imaging*, 9(2), pp. 101-109.
 11. Daubechies, I. (1998). Recent Results in Wavelet Applications, *Journal of Electronic Imaging*, 7(4), pp. 719-724.
 12. Wang, K. and Li, X. (1999). Use of Digital Cameras for Pavement Surface Distress Survey, *Transportation Research Record*, No. 1675, pp. 91-97.
 13. Fukuhara, T., Terada, K., Nagao, M., Kasahara, A., and Ichihashi, S. (1990). Automatic Pavement-Distress-Survey System, *Journal of Transportation Engineering*, 116(3), pp. 280-286.
 14. Zhou, J., Huang, P.S., and Chiang, F.P. (2006). Wavelet-Based Pavement Distress Detection and Evaluation, *Optical Engineering*, 45(2), pp. 027007-027010.
 15. Zhou, J., Huang, P., and Chiang, F.P. (2005). Wavelet-Based Pavement Distress Classification, *Transportation Research Record*, No. 1940, pp. 89-98.
 16. Chambon, S., Subirats, P., and Dumoulin, J. (2009). Introduction of a Wavelet Transform Based on 2d Matched Filter in a Markov Random Field for Fine Structure Extraction, *Application on Road Crack Detection*, San Jose, California, USA.
 17. Tsai, Y.C., Kaul, V., and Mersereau, R.M. (2010). Critical Assessment of Pavement Distress Segmentation Methods, *Journal of Transportation Engineering*, 136(1), pp. 11-19.
 18. Zhou, J., Huang, P.S., and Chiang, F.P. (2005). Wavelet-Based Pavement Distress Image Compression and Noise Reduction, San Diego, CA, USA.
 19. Canny, J. (1986). A Computational Approach to Edge Detection, *IEEE Transactions on Pattern Analysis and Machine Intelligence*, PAMI-8(6), pp. 679-698.
 20. Mallat, S. and Zhong, S. (1992). Characterization of Signals from Multiscale Edges, *IEEE Transactions on Pattern Analysis and Machine Intelligence*, 14(7), pp. 710-732.
 21. Schafer, R.W. and Rabiner, L.R. (1973). A Digital Signal Processing Approach to Interpolation, *Proceedings of the IEEE*, 61(6), pp. 692-702.
 22. Smith, M., and Barnwell, T. (1984). A Procedure for Designing Exact Reconstruction Filter Banks for Tree-Structured Subband Coders, *IEEE International Conference on ICASSP: Acoustics, Speech, and Signal Processing*.
 23. Daubechies, I. (1993). Orthonormal Bases of Compactly Supported Wavelets II: Variations on a Theme, *SIAM J. Math. Anal.*, 24(2), pp. 499-519.
 24. Rijan, K., Day, D., and Balasubramaniam, N. (2008). Analysis of Pavement Condition Data Employing Principal Component Analysis and Sensor Fusion Techniques, *International Conference on Image Processing, Computer Vision, and Pattern Recognition*.